Eric Elzenheimer*, Helmut Laufs, Tilmann Sander and Gerhard Schmidt

Magnetoneurograhy of an Electrically Stimulated Arm Nerve

Usability of Magnetoelectric (ME) Sensors for Magnetic Measurements of Peripheral Arm Nerves

Abstract: For further development and optimization of novel uncooled magnetoelectric (ME) sensors, a better understanding of spectral power distribution and signal strength of nerve signals is of high interest. For obtaining information on these signal properties, Superconducting Quantum Interference Device (SQUID) measurements were performed at the Physikalisch-Technische Bundesanstalt (PTB) in Berlin. Signal amplitudes were subject-dependent and ranged from 17 fT to 60 fT in a frequency range from 100 Hz to 1 kHz. The required SQUID averaging time was in the range of minutes, while for current ME sensors significantly longer averaging times are expected to be necessary.

Keywords: Magnetoelectric (ME) sensors, SQUID sensors, Magnetic measurements on peripheral arm nerves, N. Medianus, Biomagnetic Applications, Magnetoneurograhy

https://doi.org/10.1515/cdbme-2018-0087

1 Introduction

Uncooled contactless magnetoelectric (ME) sensors provide an alternative technology to adhesive electrodes in biomedical applications. Within the collaborative research center 1261, several types of ME sensors are being investigated and promise a great progress in terms of sensitivity and limit of detection (LOD).

The main sensor principle is based on a polysilicon cantilever (Si), where the bottom is coated with a magnetostrictive material (FeCoSiB) and the top with a piezoelectric material (AlN) [1]. This electromechanical resonator can be used as a magnetometer, because it uses the mechanical coupling between the magnetostrictive and the piezoelectric layer in a resonant structure. A change in an external magnetic field causes a strain in the magnetostrictive component, which is directly mechanically transferred to the piezoelectric component. The resulting electrical signal from the piezoelectric material is proportional to the primary magnetic field change. The main advantage of this sensor principle is that an operation in normal (unshielded) environments without any saturation effects can be achieved. This is in contrast to competing sensor principles such as Optically-Pumped-Magnetometers [2] or SQUIDs [3]. Therefore, this ME sensor technology is also of special interest for Magnetoneurograhy (MNG), which measures human nerve magnetic fields. Currently, ME sensors only reach an LOD of about 1 pT/√(Hz) in a narrowband frequency range [4]. In previous SQUID work [5,6], field amplitudes of 10 fT to 100 fT were measured. These depended on nerve-to-sensor-distance and appeared in the typical frequency range from 100 Hz to 1 kHz [7]. Greater signal strengths should be achieved by a simultaneous electrical stimulation of afferent as well as efferent nerve fibers, which can be achieved via a “mixed nerve stimulation” procedure [8,9].

It is of interest to identify which signal strengths and spectral power distributions can be detected with MNG. Respective data will allow to determine the applicability of ME sensors for MNG.

2 Methods, Measurement Setup, Execution and Evaluation

2.1 Preliminary Examination of healthy Subjects

Multichannel electric nerve conduction studies on two healthy subjects aged 30 and 24 years (one female) were performed. First, the depth-profile of the median nerve (N. medianus) for each subject was obtained via ultrasound for each subject. Next, conducted multichannel electric measure-

***Corresponding author: Eric Elzenheimer,** Kiel University, Digital Signal Processing and System Theory, Kaiserstr. 2, 24143 Kiel, Germany
E-mail:eric.elzenheimer@tf.uni-kiel.de
Helmut Laufs: UKSH, Department of Neurology, Arnold-Heller-Str. 3, 24105 Kiel, and Kiel-University, Kiel, Germany
Tilmann Sander-Thömmes: Physikalisch-Technische Bundesanstalt (PTB), Abbestr. 2-12, 10587 Berlin, Germany
Gerhard Schmidt: Kiel University, Digital Signal Processing and System Theory, 24143 Kiel, Germany

ments focusing on the upper arm in order to keep the greatest possible distance between the palmar stimulation and the recording site were performed (Fig. 1). This setup allow a temporal separation between the stimulation artefact and the induced biological nerve signal (Figs. 1 and 2). For recording of electrical signals a clinical CE certified electroneurography system was used (Nicolet EDX-System from Natus Medical). A unipolar rectangular pulse of 15 mA with a duration of 200 µs was applied in the vicinity of the musculus abductor pollicis brevis (APB), such that both motor and sensory fibers were excited simultaneously. While ensuring a stable skin temperature above T = 30 °C for each subject mixed nerve action potentials (NAP) at the different positions along the nerve were obtained via three repetitions. In the next paragraph, the magnetic measurements setup and execution are described.

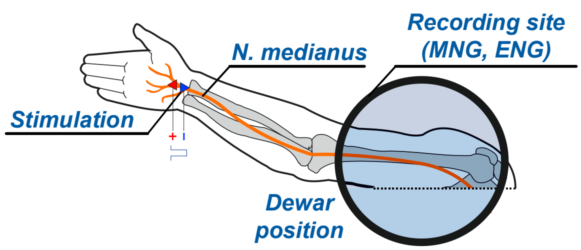

Figure 1: Illustration of stimulation and recording site for electrical (ENG) as well as magnetical (MNG) measurement.

2.2 Measurement Setup and Execution

The MNGs were performed within the active and passive magnetically shielded chamber (BMSR-2) [10] using a 304-SQUID vector magnetometer system [11]. Subjects were prone positioned on a non-magnetic patient bench in BMSR-2. The SQUID dewar was centered and aligned above and with a direct skin contact to the upper arm (Fig. 2). The distance between nerve and skin was 1.54 cm for subject 1 and 0.88 cm for subject 2. The SQUID system ensures a total noise level of about 2.3 fT/√(Hz) at 1 kHz within a frequency range of 100 Hz - 10 kHz [12]. However, with this high sensor sensitivity, a direct signal detection of the nerve impulses is not ensured, because in addition to sensor noise, biological interferences e.g. from the heart and muscle magnetic fields occur. By means of unweighted averaging triggered by an electrical stimulation pulse, the signal-to-noise ratio (SNR) could be improved proportionally to the root of the number of averaging periods. Therefore, the stimulus-synchronous trigger signal of the stimulator is recorded simultaneously to the SQUID signals. The same stimulation as in the preliminary subject examination was applied with a stimulation rate of 8.547 Hz as a compromise between subject comfort and duration of the experiment. This results in a total measurement time for each subject smaller than 30 min. In addition to and simultaneously with the MNG, again electrical nerve measurements were performed in analogy to those described in Sec. 2.1 using an custom built amplifier by the PTB specifically for use in the magnetically shielded chamber.

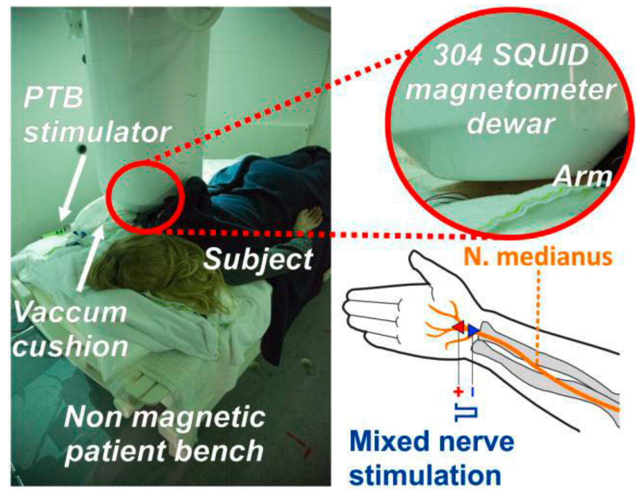

Figure 2: Real measurement setup with subject positioned under SQUID vector magnetometer system.

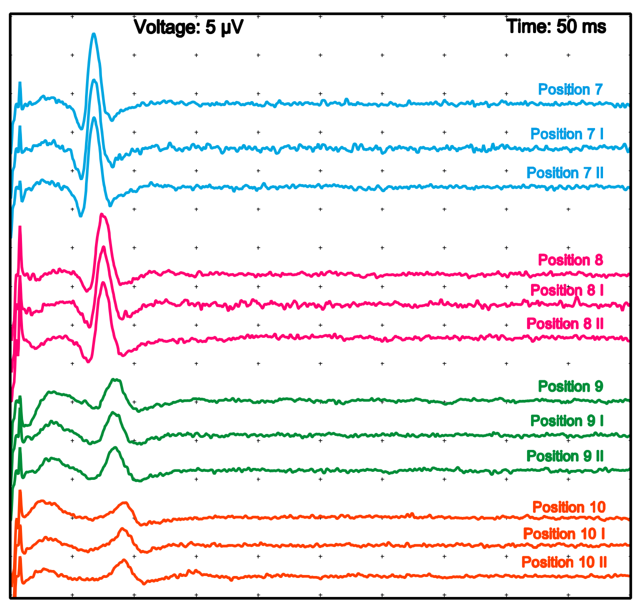

Figure 3: Multichannel ENG of subject 1 in the upper arm area of n. medianus with a $sNCV_{Mean}$ of 61 m/s. Traces are recorded by a Y-axis shift for separation purposes. Amplitude (5µV/DIV) and Time scaling (50 ms/DIV) is constant for all recordings.

2.3 Signal Processing and Evaluation

The multichannel electric nerve conduction studies in combination with ultrasound resulted in a finer grained functional-spatial reference characterization of the nerve. Fig. 3 displays an example multichannel measurement from subject 1. Furthermore, the mean segmental nerve conduction velocity (sNCV) of the individual subjects could be consistently determined. Subject 1 achieved a sNCV of 61 m/s and subject 2 a sNCV of 51 m/s. These values lie in the standard range according to [9]. For the magnetic measurements, MNG signals of the Z-SQUID-Modules (1^{st} sensor level) focussing on the most distal measurement position were analysed. This is the position closest to the stimulation site, i.e. 35 cm for both subjects. The signals were recorded with a sampling frequency f_S = 10 kHz and filtered with two Bessel filters (high-/low-pass filter of order N_{Filt} = 8, f_{Cut} = 5 Hz / 1.5 kHz). A linear trend removal and an unweighted averaging to further optimise the SNR were performed. From the simultaneously recorded trigger, signal stimulation time positions could be precisely extracted and transferred into the vector

$$\boldsymbol{m} = \left[m_1 \ldots m_i \ldots m_N\right], \tag{1}$$

where the amount of averaging periods is defined by N. Individual averaging epochs could be determined through the available start indices and by taking the trigger times as zero point of the individual epochs. A constant epoch duration of 30 ms was chosen including pre- and poststimulus intervals of 10 ms ($K_{Pre} = 10\ ms{\cdot}f_S$) and 30 ms ($K_{Post} = 30\ ms{\cdot}f_S$), respectively. Based on the trigger signal, individual epochs were derived from the individual SQUID signals $x_{MNG}(n)$, described by the vector

$$\boldsymbol{x}_{EP}\left(u\right) = \left[x_{MNG}\left(m_u - K_{Pre}\right) \ldots x_{MNG}\left(m_u + K_{Post}\right)\right]^T \quad \forall u = 1\mathrm{K}\ N. \tag{2}$$

$K_{Pre}+K_{Post}+1$ is the buffer length for the averaging process. The averaging finally results in:

$$\bar{\boldsymbol{s}}_m\left(N\right) = \frac{1}{N} \cdot \sum_{l=1}^{N}\left(\boldsymbol{x}_{EP}\left(l\right)\right) \tag{3}$$

The results for each subject are presented in Fig. 4.

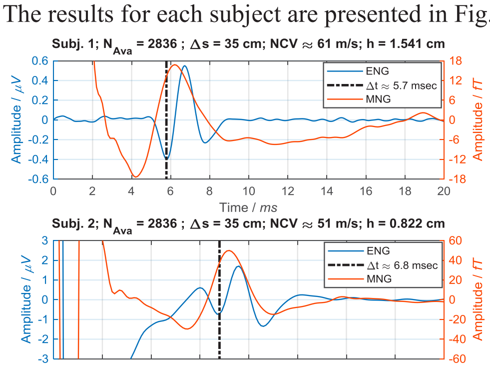

Figure 4: Final results of the MNG measurements averaged over 2836 stimulations.

It is to be noted that the sNCV obtained in the electrical and the magnetic measurements are identical. The MNG amplitudes were 16.81 fT (*subject 1*) and 49.96 fT (*subject 2*). The spatial distribution of the magnetic field as a function of time was consistent with a propagating nerve impulse (not shown) and supports the interpretation of the magnetic peaks in Fig. 3 between 4-8 ms (*subject 1*) and between 6-10 ms (*subject 2*) as nerve signals. Furthermore, an additional influence by F-Waves [13] can be excluded due to the very small signal delay and the chosen stimulation frequency.

3 Simulation

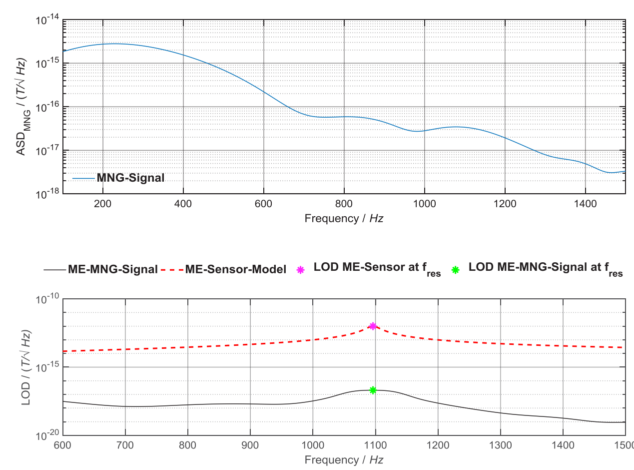

Figure 5: Amplitude Spectral Density and ME Sensor LOD to determine the applicability of ME sensors

The amplitude densities displayed in Fig. 5 are the result of simulations based on the maximum flux density of the second subject (49.96 fT; cf. Fig. 4) and a simplified ME sensor model. An amplitude response of an ME sensor (without equalization) can be based on a digital bandpass filter with a bandwidth of 20 Hz and a resonance frequency of 1096 Hz (electromechanical resonator behavior). The first resonance frequency of ME sensors appears at approximately 1 kHz for the first mode [1]. The resonance frequency as well as the bandwidth, can be adjusted by the thickness and dimension of the sensor substrate. The simulation shows that an averaging time of $5{\cdot}10^6$ min would be necessary to achieve an SNR of 0 dB in resonance (f_{Res}) with an LOD of 1 pT/√(Hz), see Fig. 5.

4 Conclusion and Outlook

The results show that it is possible to perform MNGs using the mixed nerve stimulation method described in 2.1. Using the described digital signal preprocessing and unweighted averaging, meaningful sNCV and NAP resulted based on data with a recording time of no longer than 6 minutes. The reduction of the Dewar surface-to-skin-distance below 15 mm [12] should further increase the nerve signal amplitude by the change in distance to the power of three [14]. However, the simulations presented in Fig. 4 illustrate that an MNG with the help of ME sensor technology is not feasible at the current state of development, especially if an SNR > 0 dB shall be achieved within a reasonable averaging time.

The bandwidth of MNGs lie in the frequency range between 100 Hz and 1 kHz, which also require a larger mandatory sensor detection bandwidth. In the next step, MNG signal analysis can be further improved by capitalizing on additionnal SQUID sensor signals, i.e. by a spatial comparison. This is achievable, because additional marker coils were placed at the individual subjects during MNG and their positions were recorded by an ultrasound-based motion analysis system (CMS 20 Zebris Medical GmbH).

In addition, it is interesting to investigate, whether a further reduction of the averaging time is possible by using adaptive averaging in the time-frequency domain. In future, the focus of ME sensor development could be set on the magnetic measurement of muscle action potentials, which exhibit a magnetic signal amplitude 10 to 1000 times higher than that of the nerve action potential.

Acknowledgment: We gratefully acknowledge the financial support for CRC 1261 "Magnetoelectric Sensors: From Composite Materials to Biomagnetic Diagnostics" of German Research Foundation (Deutsche Forschungsgemeinschaft, DFG). The MNG measurements was made possible by the DFG funding of "Metrology of Ultra-Low Magnetic Fields". Special thanks to Franziska Weitkamp and Sebastian Engel (UKSH) for the additional support.

Author Statement

Research funding: This work was funded by the German Research Foundation (Deutsche Forschungsgemeinschaft, DFG) through the Collaborative Research Centre CRC 1261 Magnetoelectric Sensors: From Composite Materials to Biomagnetic Diagnostics. Conflict of Interest: Authors state no conflict of interest. Informed consent: Informed consent has been obtained from all the individuals included in this study. Ethical approval: The research related to human use complies with all the relevant national regulations, institutional policies and was performed in accordance with the tenets of the Helsinki Declaration, and has been approved by the authors' institutional review board or equivalent committee.

References

[1] Yarar, E. et al. (2016): Inverse bilayer magnetoelectric thin film sensor. In: Appl. Phys. Lett. 109 (2), S. 22901.

[2] Boto, Elena; Meyer, Sofie S.; Shah, Vishal; Alem, Orang; Knappe, Svenja; Kruger, Peter et al. (2017): A new generation of magnetoencephalography: Room temperature measurements using optically-pumped magnetometers. In: NeuroImage 149, S. 404–414.

[3] Körber, R. et al. (2016): SQUIDs in biomagnetism. A roadmap towards improved healthcare. In: Supercond. Sci. Technol. 29 (11), S. 113001.

[4] Röbisch, V. et al. (2015): Exchange biased magnetoelectric composites for magnetic field sensor application by frequency conversion. In: Journal of Applied Physics 117 (17), 17B513

[5] Trahms, L. et al. (1989): Biomagnetic functional localization of a peripheral nerve in man. In: Biophysical journal 55 (6), S. 1145–1153.

[6] Mackert, B. et al. (2004): Magnetoneurography. Theory and application to peripheral nerve disorders. In: Clinical neurophysiology: official journal of the International Federation of Clinical Neurophysiology 115 (12), S. 2667–2676.

[7] Sternickel, K.; Braginski, Alex I. (2006): Biomagnetism using SQUIDs. Status and perspectives. In: Supercond. Sci. Technol. 19 (3), S160-S171.

[8] Buschbacher, R. M. (1999): Mixed nerve conduction studies of the median and ulnar nerves. In: American journal of physical medicine & rehabilitation 78 (6 Suppl), S69-74.

[9] Weitkamp, F. et al.: Multimodal Mapping of Nerve Pathology with a Multichannel Approach, DKGN 2017, 2017.

[10] Watson, J. et al. (2002): Mixed median nerve forearm conduction velocity in the presence of focal compression neuropathy at the wrist versus peripheral neuropathy. In: Archives of physical medicine and rehabilitation 83 (3), S. 302–307.

[11] Bork, J.; Hahlbohm, H.-D.; Klein, R.; Schnabel A.: The 8-layered magnetically shielded room of the PTB: Design and construction, Biomag 2000, Helsinki, 2000

[12] Burghoff, M.; Schnabel, A.; Drung, D.; Thiel, F.; Knappe-Grüneberg, S.; Hartwig, S. et al. (2004): Discrimination of multiple sources using a SQUID vector magnetometer. In: Neurology & clinical neurophysiology: NCN 2004, S. 67.

[13] Guiloff, Roberto J. (2006): Chapter 9 Late responses (F- and A-waves). Methodology and techniques. In: Jun Kimura (Hg.): Peripheral nerve diseases, Bd. 7: Handbook of Clinical Neurophysiology, v. 7) S. 189–235.S.

[14] J. Williamson, M. Hoke, G. Stroink, M. Kotani: Advances in Biomagnetism, Proceedings of the Seventh International Conference on Biomagnetism, Plenum Press, New York, 1989